Eur. Phys. J. D **6**, 201–209 (1999)

THE EUROPEAN PHYSICAL JOURNAL D

EDP Sciences

Molecular dissociative sequential excitation and ionization of strontium vapor

M.A. Baig[1,a], M. Yaseen[1], Raheel Ali[1], Ali Nadeem[2], and S.A. Bhatti[2]

[1] Atomic and Molecular Physics Laboratory, Department of Physics, Quaid-i-Azam University, Islamabad 45320, Pakistan

[2] Applied Physics Division, PINSTECH, P. O. Box Nilore, Islamabad, Pakistan

Received: 10 September 1998 / Received in final form: 16 December 1998

Abstract. We report new measurements on laser-assisted molecular dissociative sequential excitation and ionization spectra of strontium vapor. A single Nd:YAG pumped dye laser in conjunction with an atomic beam apparatus have been used to investigate the even parity $5snd\ ^{3,1}D_2$ Rydberg series resulting from the $5s5p\ ^1P_1$ resonance level. The relative intensities changes among the $5snd\ ^3D_2$ and $^1D_2$ Rydberg series are attributed to the interactions with the $4d6s\ ^{1,3}D_2$ perturbers, respectively. The interchannel interactions between the $5snd\ ^1D_2$ series and the $4d6s\ ^1D_2$ level and among the $5snd\ ^3D_{1,2,3}$ series and the $4d6s\ ^3D_{1,2,3}$ intruders have been separately parameterized using the two-channel quantum defect theory.

PACS. 31.50.+w Excited states 32.30.Jc Visible and ultraviolet spectra 32.80.Rm Multiphoton ionization and excitation to highly excited states (e.g., Rydberg states)

1 Introduction

The highly excited Rydberg states of strontium have been extensively investigated using conventional spectroscopy [1,2] and laser spectroscopy ([3–5] and references therein). The even parity states were first studied by Ewart and Purdie [6] using a nitrogen pumped dye laser in conjunction with a thermionic diode. They reported the $5sns\ ^1S_0$ ($10 \leq n \leq 19$), $5snd\ ^1D_2$ ($9 \leq n \leq 35$) and $5snd\ ^3D_2$ ($24 \leq n \leq 33$) series. Subsequently, Esherick [7] reported the $5sns\ ^1S_0$ ($10 \leq n \leq 21$), $5snd\ ^1D_2$ ($9 \leq n \leq 60$) and $5snd\ ^3D_2$ ($9 \leq n \leq 37$) series in addition to a strong autoionizing resonance about 450 cm^{-1} above the first ionization threshold. A five-channel quantum defect theory was used to parameterize the interactions among the $J = 2$ channels. The g-factors for the $5snd\ J = 2$ series, in the perturbed region ($11 \leq n \leq 20$), were measured by Wynne *et al.* [8] using multiphoton ionization spectroscopy and it was inferred that the variation of the g-factors is in accord with the MQDT predictions. Rubbmark and Borgstrom [9] reported an extensive study of the Rydberg series in strontium using one laser to selectively excite the atoms to a particular state and the second broad band laser was used as a continuum background to photograph the absorption spectra. The triplet series, $5sns\ ^3S_1$ ($11 \leq n \leq 45$), $5snd\ ^3D_1$ ($12 \leq n \leq 32$), $5snd\ ^3D_2$ ($12 \leq n \leq 40$) and $5snd\ ^3D_3$ ($12 \leq n \leq 45$), were studied by Beigang *et al.* [10] *via* the discharge population of the metastable states $5s5p\ ^3P_{0,1,2}$ and subsequent excitation by the frequency doubled tunable dye laser in conjunction with a thermionic diode. Beigang *et al.* [11] studied the influence of singlet-triplet mixing on the hyperfine structure of the $5snd$ series and the natural lifetimes of these series were reported by Grafstrom *et al.* [12]. The interchannel interactions of the triplet series $J = 1$ and $J = 3$ were analyzed by Beigang and Schmidt [13] using a two-channel approach. All the experiments cited above were performed using a heat pipe for the vapor containment and a thermionic diode as an ion detector. Recently, Dai [14,15] reinvestigated the $5sns\ ^1S_0$ series and the perturbed $5snd\ ^{1,3}D_2$ Rydberg series in strontium using an isolated core excitation technique in conjunction with an atomic beam apparatus. Dai [15] also performed the multi-channel quantum defect theory analysis to describe the inter-channel interactions, a two-channel model for the triplet terms and a three-channel model for the singlet terms.

In the present paper, we report the measurements on $5snd\ ^{1,3}D_2$ series by the molecular dissociative sequential excitation from the $5s5p\ ^1P_1$ resonance level. The $5sns\ ^1S_0$ series is too weak to be observed revealing only the $5snd\ ^{1,3}D_2$ series. The intensity variation among the singlet and triplet series is attributed to the interactions with the $4d6s\ ^{1,3}D_2$ levels. It is shown that, as in the case of $5snd\ ^3D_{1,3}$ series, a two-channel model is sufficient to describe the interactions of the singlet and triplet series with the corresponding perturbers. To get a consistent picture of the interchannel interactions, we present here the MQDT analysis of all four $5snd\ ^1D_2$, $^3D_{1,2,3}$ series interacting with the corresponding $^1D_2$, $^3D_{1,2,3}$ perturbing levels pertaining to the $4d6s$ configuration.

[a] e-mail: Baig@physics.sdnpk.undp.org

2 Experimental details

A tunable Hänsch type [16] dye laser with a bandwidth of about 0.3 cm^{-1}, pulse width 5-6 nsec and pumped by a 10 Hz repetition rate Nd: YAG (Spectra Physics GCR 11-2D) laser was used to carry out the experiment. The THG (Third Harmonic Generation) at 355 nm with pulse energy of 20 mJ was used to pump the dye laser operated with C-500 dye dissolved in ethanol. The dye laser was tuned by a computer controlled stepper motor over the wavelength region from 460 nm to 410 nm.

An atomic beam of strontium was produced by means of a resistively heated oven with $\approx$ 0.2 mm aperture. The atomic beam was crossed by the dye laser beam at right angle to the atomic beam between a pair of stainless steel plates, 5 $\times$ 5 cm, 1 cm thick and spaced 1 cm apart. The photons in the laser pulse used to excite the atoms were energetic enough to photoionize the resulting excited atoms. Consequently, the Rydberg atoms could be photoionized by photons of the same laser pulse. The ions were collected by a very weak electric field about 1 volt/cm and were detected using a channeltron placed above the 1 cm hole in the top plate covered with a fine thin mesh. No electric field pulse across the interaction region was used to field ionize the Rydberg atoms so that to observe only the photoionization of the Rydberg states.

The output beam of the dye laser was focused into the interaction region by a 100 cm focal length quartz lens. The output laser beam from the chamber was divided into two parts by a 50/50 beam splitter to record the etalon fringes and the optogalvanic signal from an argon hollow cathode. Three independent detection channels have been used to record the data. The signals from the channeltron, the hollow cathode and the solid etalon were sampled simultaneously by three separate boxcar integrators (SR 250) and stored on the PC for subsequent analysis.

3 Results and discussion

A schematic energy level diagram of strontium atom and the potential energy curves for the ground state and the first excited state of the strontium molecule Sr_2 are shown in Figure 1. Using a single dye laser covering the wavelength from 460 to 410 nm, we have observed the even parity $5snd\ ^{3,1}D_2$ Rydberg series originating from the $5s5p\ ^1P_1$ resonance level. Figure 2 shows the spectra obtained while scanning the laser between 21800 cm^{-1} to 23000 cm^{-1}. In this figure the lines are identified due to two different excitation mechanisms: two-photon excitation from the ground state and sequential excitation from the $5s5p\ ^1P_1$ level. In particular, the $5s9d\ ^3D_2$ level is observed at 21877.9 cm^{-1} due to two-photon excitation, whereas it is observed at 22106.4 cm^{-1} due to sequential excitation. The difference in their energies is about 228.5 cm^{-1}. Looking at their relative intensities, the transitions due to the two-photon excitation are much stronger than due to the excitation from the $5s5p\ ^1P_1$ level. The $5s9d\ ^3D_2$ level is about nine times stronger in two-photon

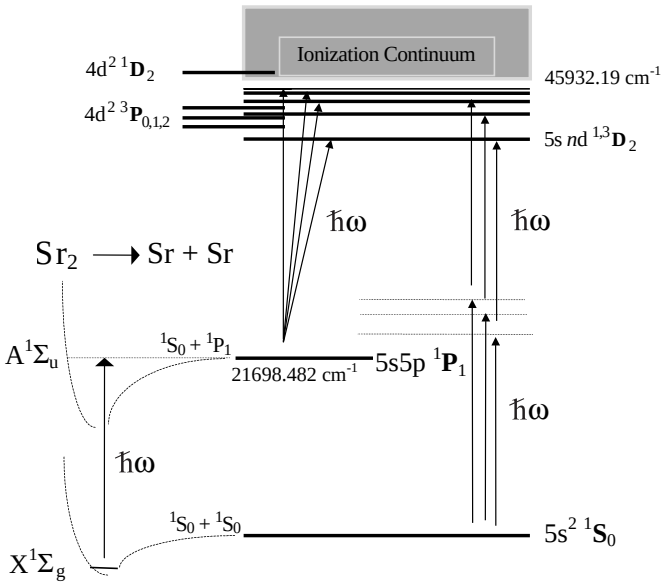

Fig. 1. Schematic energy level diagram of strontium showing the direct two-photon excitation from the ground state and the sequential excitation from the $5s5p^1P_1$ level. The molecular state of strontium dimer is also shown to clarify the population of the $5s5p\ ^1P_1$ level due to the dissociation of Sr_2 to one Sr atom in the $5s^2\ ^1S_0$ level and the other in the $5s5p\ ^1P_1$ excited level.

excitation as compared to that in the sequential excitation. This shows that the population of the $5s5p\ ^1P_1$ level is not very high. An important point is that the transitions to the $4d^2$ configuration based levels have been also observed due to both the above-mentioned excitation processes. In particular, the $4d^2\ ^3P_0$ and $^3P_2$ levels are observed at 22263.2 cm^{-1} and 22365.2 cm^{-1} due to the two-photon excitation from the ground state (see Fig. 2) and at 22827.1 cm^{-1} and 23030.9 cm^{-1}, respectively, due to the excitation from the $5s5p\ ^1P_1$ level. The third component of this multiplet $4d^2\ ^3P_1$ is observed at 22896.5 cm^{-1} only via the excitation from the $5s5p\ ^1P_1$ level as it is not allowed in two-photon excitation due to the ΔJ selection rule. The identifications of the other lines are marked in these figures. The observed and the expected excitation energies, from the known literature values, of these transitions are tabulated in Table 1.

A portion of the spectrum covering the laser photon energy from 22750 cm^{-1} to 24250 cm^{-1} is shown in Figure 3. A sequence of Rydberg series in addition to a dominating autoionizing resonance is evident, although no Rydberg series was expected in this region except the one $(4d^2+5p^2)\ ^1D_2$ autoionizing resonance at 23190 cm^{-1}. To understand the observed structure, we have to consider all the possible mechanisms that are contributing to the excitation in this energy region. Since the laser photon energy extends from 22750 cm^{-1} to 24250 cm^{-1}, only the structure due to two-photon excitation from the $5s^2\ ^1S_0$ ground state can occur with a series limit at 22966 cm^{-1}. The second contribution in the structure may arise from the one-photon excitation from the $5s5p\ ^1P_1$ resonance level,

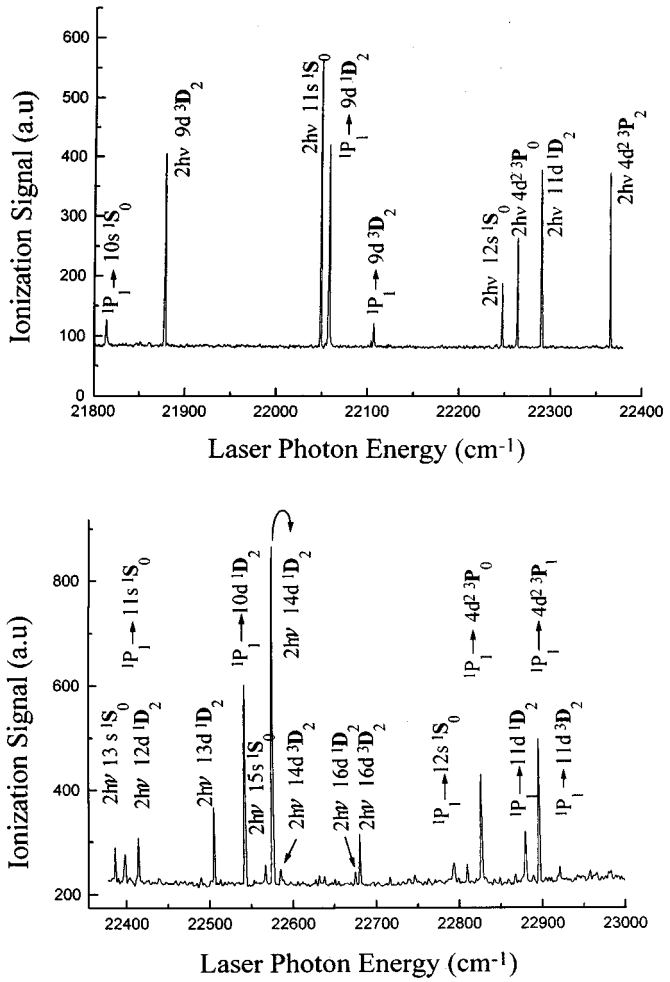

Fig. 2. Discrete structure in the laser photon energy from 21800 cm^{-1} to 23000 cm^{-1} due to two-photon excitation from the ground state and sequential excitation from the collisionally populated $5s5p\ ^1P_1$ resonance levels. The term energies of each level have been determined accordingly whereas the excitation laser energies are given in Table 1.

provided this level is substantially populated by some possible mechanisms (see below for explanation). The third possibility is the excitation to the autoionizing levels built on the $4d(^2D_{3/2,5/2})$ or $4p(^2P_{1/2,3/2})$ ionic levels of strontium. Again it must be due to the two-photon excitation from the ground state taking into account that the laser photon energy is slightly higher than the $5s5p\ ^1P_1$ level.

To explain the observed structure shown in Figure 3, we start from the lower energy side of the trace. In addition to four lines (for their identifications see Table 1), there is a clear jump in the ionization signal around 22966 cm^{-1} that corresponds to the first ionization threshold (two-photon) of strontium. Above this step in the ionization signal, a relatively strong and sharp line at 23030.9 cm^{-1} is identified as $5s5p\ ^1P_1 \rightarrow 4d^2\ ^3P_2$ and the strong autoionizing resonance at 23190 cm^{-1} is identified as a two-photon excitation from the ground state to the $(4d^2+5p^2)\ ^1D_2$ level. Since this is the only level, which energetically lies above the first ionization threshold, it can decay into the $5s\varepsilon\ell$ adjacent continuum revealing a Fano type [17] autoionizing resonance line shape.

The origin of the appearance of these resonances becomes clear from the energy level diagram of strontium atom and the strontium molecule Sr_2 (see Fig. 1). These resonances correspond to transitions between the excited $5s5p\ ^1P_1$ level and the $5snd\ ^1D_2$ and $5snd\ ^3D_2$ Rydberg series converging around 24250 cm^{-1}. These resonances appear in the two-photon excitation experiment when the laser is scanned from 22900 to 24250 cm^{-1}. Since the $5s5p\ ^1P_1$ level is at 21698.482 cm^{-1} [18], the detuning from the nearest real level is about 1200 cm^{-1} for the two-photon excitation. The mechanism for the $5s5p\ ^1P_1$ population is the excitation of the strontium molecules, which are always present in an atomic beam, into a dissociating state. The $X^1\Sigma_g$ ground state of the strontium molecule

Table 1. The $5s10d\ ^1D_2$ line is too weak to be observed via two-photon excitation from the ground state but observed with a reasonable intensity from the $5s5p^1P_1$ level at 22543.1 cm^{-1}. The term energies for the upper levels can be calculated by doubling the listed laser energies for the two-photon transitions and by adding 21698.482 cm^{-1} [18] to the laser photon energy for the transition from the $5s5p\ ^1P_1$ level.

Excitation Energy		Level Assignments
Observed	Expected	
21813.7	21813.5	$5s5p\ ^1P_1 \rightarrow 10s\ ^1S_0$
21877.8[a]	21877.9	$5s^2\ ^1S_0 \rightarrow 9d\ ^1D_2$
22048.2[a]	22048.4	$5s^2\ ^1S_0 \rightarrow 11s\ ^1S_0$
22057.5	22057.4	$5s5p\ ^1P_1 \rightarrow 9d\ ^1D_2$
22106.2	22106.4	$5s5p\ ^1P_1 \rightarrow 9d\ ^3D_2$
22246.5[a]	22246.4	$5s^2\ ^1S_0 \rightarrow 12s\ ^1S_0$
22263.2[a]	22262.9	$5s^2\ ^1S_0 \rightarrow 4d^2\ ^3P_0$
22289.4[a]	22289.3	$5s^2\ ^1S_0 \rightarrow 11d\ ^1D_2$
22365.2[a]	22364.3	$5s^2\ ^1S_0 \rightarrow 4d^2\ ^3P_2$
22386.7[a]	22386.7	$5s^2\ ^1S_0 \rightarrow 13s\ ^1S_0$
22398.3	22398.3	$5s5p\ ^1P_1 \rightarrow 11s\ ^1S_0$
22414.8[a]	22414.7	$5s^2\ ^1S_0 \rightarrow 12d\ ^1D_2$
22505.7[a]	22505.8	$5s^2\ ^1S_0 \rightarrow 13d\ ^1D_2$
22543.1	22543.2	$5s5p\ ^1P_1 \rightarrow 10d\ ^1D_2$
22567.2[a]	22567.4	$5s^2\ ^1S_0 \rightarrow 15s\ ^1S_0$
22575.4[a]	22576.5	$5s^2\ ^1S_0 \rightarrow 14d\ ^1D_2$
22680.7[a]	22681.0	$5s^2\ ^1S_0 \rightarrow 16d\ ^1D_2$
22827.1	22827.3	$5s5p\ ^1P_1 \rightarrow 4d^2\ ^3P_0$
22879.8	22880.1	$5s5p\ ^1P_1 \rightarrow 11d\ ^1D_2$
22896.5	22897.5	$5s5p\ ^1P_1 \rightarrow 4d^2\ ^3P_1$
23030.9[b]	23031.1	$5s5p\ ^1P_1 \rightarrow 4d^2\ ^3P_2$
23190[c]		$5s^2\ ^1S_0 \rightarrow (4d^2+5p^2)^1D_2$

[a] Two-photon transition from the ground state.
[b] Strong line.
[c] Strongly autoionizing resonance, FWHM is about 57 ± 1 cm^{-1}.

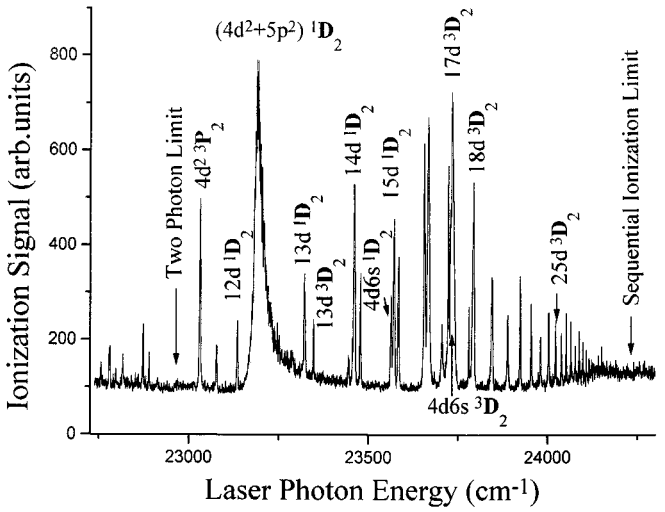

Fig. 3. Spectra covering the laser photon energy from 22850 cm^{-1} to 23850 cm^{-1} showing the $5snd\ ^{1,3}D_2$ Rydberg series excited from the $5s5p\ ^1P_1$ level. The dominating autoionizing resonance is due to direct two-photon excitation from the ground state $(4d^2 + 4p^2)\ ^1D_2$. This autoionizing resonance was fitted to the two-channel MQDT relation to determine the width $\Gamma = 57 \pm 1$ cm^{-1}. Due to the absence of the $5sns\ ^1S_0$ series the intensity variation among the singlet and triplet series is worth noting.

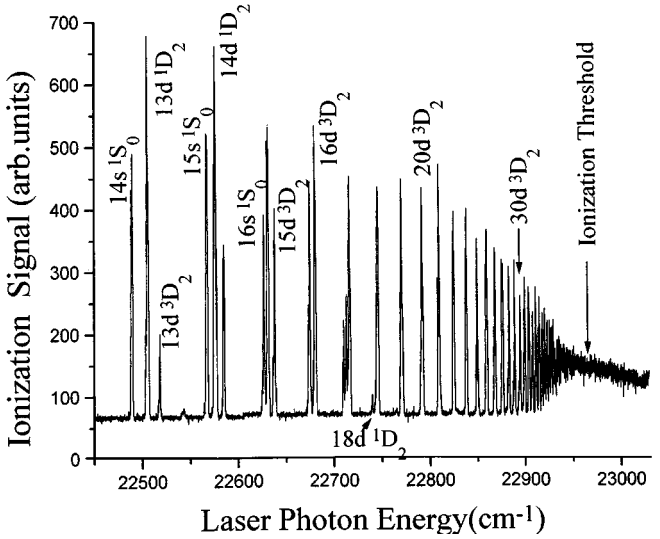

Fig. 4. Spectra covering the laser photon energy 22400-23030 cm^{-1}, recorded using the thermionic diode ion detector, showing clearly the $5sns\ ^1S_0$ and $5snd\ ^{1,3}D_2$ series.

arises from two ground-state strontium atoms. This molecular state is only weakly bound with dissociation energy of about 1088 cm^{-1}, as has been recently calculated by Boutassetta *et al.* [19]. The Sr_2 molecule absorbs a photon and is excited to the dissociation continuum of the $A^1\Sigma_u$ state which leads to the dissociation into two strontium atoms, one in the ground state Sr $(5s^2\ ^1S_0)$ and the other in the first excited state $Sr^*(5s5p\ ^1P_1)$.

$$Sr_2X\ ^1\Sigma_g \rightarrow (Sr_2)^* \rightarrow Sr(5s5p\ ^1P_1) + Sr(5s^2\ ^1S_0)\,.$$

Since the dissociation process is very fast ($\approx 10^{-12}$ s), it is possible that the atoms in the $5s5p\ ^1P_1$ excited state absorb a second photon from the same laser pulse ($\approx 5 \cdot 10^{-9}$ s) which leads to the excitation of the observed Rydberg series, $5s5p\ ^1P_1 \rightarrow 5snd\ ^{1,3}D_2$. The atoms in these excited states are then ionized either by absorbing another photon from the same laser pulse or due to the black body radiation [20]. The process is termed as sequential excitation since similar excitations have been observed in alkali atoms [21–24].

Incidentally, this portion of the spectrum (see Fig. 3) covers the region where the $5snd\ ^{1,3}D_2$ series exhibit strong perturbations. An interesting observation in this part of the spectrum is the relative intensities of the $5snd\ ^1D$ and ^3D $J = 2$ levels. At $n = 13$ and 14 the $^1D_2$ line is stronger than the $^3D_2$ line. A new line emerges at the lower-energy side and adjacent to the $n = 15$ multiplet. The relative intensities of the singlet and triplet remain the same but the width of the lower-energy component $^1D_2$ increases. At $n = 16$, both of these components possess nearly identical intensities but the width of the higher-energy side component $^3D_2$ increases by 50%. Since, only the $5snd\ ^1D_2$ series exhibits this perturbation, the responsible interloper may be assigned as $4d6s\ ^1D_2$. The $4d6s\ ^3D_2$ interloper emerges adjacent to the $5s17d\ ^3D_2$ level resulting in a much broader $5s17d\ ^3D_2$ line but the $5s17d\ ^1D_2$ line retains its sharpness. At $n = 18$, the $5snd\ ^1D_2$ line becomes almost three times weaker than the $^3D_2$ line and, subsequently, at $n \geq 19$ only one line remains that forms a convergence of the Rydberg series around 24250 cm^{-1}. An important point to remember in this region is that the $5sns\ ^1S_0$ series remains too weak to be detected, therefore, the identification of the Rydberg series as $5snd\ ^{1,3}D_2$ is unambiguous. The weak intensities of the $5sns\ ^1S_0$ series can be attributed to the transition probabilities that are higher in the case when $\Delta\ell$ and ΔJ change in the positive direction, as in the case of transitions from $5s5p\ ^1P_1$ to $5snd\ ^{1,3}D$ ($\Delta\ell = \Delta J = \Delta L = +1$) as compared to the transition to the $5sns\ ^1S_0$ levels ($\Delta\ell = \Delta J = \Delta L = -1$).

Recently, Dai [15] reported the same structure using a rather complicated three-laser setup for an isolated core excitation scheme. Comparing their Figure 2 with the present data (Fig. 3), it shows an identical intensity distribution among the $5snd\ ^3D_2$ and $^1D_2$ lines.

The absence of the $5sns\ ^1S_0$ series in the sequential excitation from the $5s5p\ ^1P_1$ level eliminates, to certain extent, the possibilities of misinterpretation of the lines because this series appears strongly in the heat pipe based experiments (two-photon excitation) [6,7]. We have also repeated this experiment using a thermionic diode detector (for experimental details see Baig *et al.* [24]). The spectrum is shown in Figure 4 that clearly demonstrates the immediate difference between the atomic beam data (sequential excitation) and the thermionic diode based experiments (two-photon excitation). The spectrum shows ionization peaks forming sequences of the $5snd\ ^{1,3}D_2$ and

$5sns\ ^1S_0$ Rydberg series. Since the spectral power output of the Rydberg laser does not vary appreciably over the wavelength range and the ion detector is also linear, the peak height in the ionization signal represents approximately n-dependence of the cross-section.

The abrupt disappearance of the $5sns\ ^1S_0$ series is worth noting because it is almost impossible to identify this series at and after $n = 16$, even the identification of $5s16s\ ^1S_0$ becomes doubtful if we compare the data with that of the atomic beam experiment (see Fig. 3). The interpretations of the multiplet around 23570 cm^{-1} (see Fig. 3) have always attracted much attention in the past. Ewart and Purdie [6] identified the lower-energy component as $4d6s\ ^3D_2$, the middle one as $5s16s\ ^1S_0$ and the higher-energy side component as $5s15d\ ^1D_2$, whereas, Esherick [7] identified the first line $5s16s\ ^1S_0$, and the other two lines were assigned as a mixture of $5s15d\ ^{1,3}D_2$ levels. Since in the present work, there are three clearly resolved lines, and the $5sns\ ^1S_0$ series is too weak to be observed, the identification of the first line as $5s16\ ^1S_0$ can be ruled out. The identification of this multiplet is, therefore, $4d6s\ ^1D_2$, $5s15d\ ^1D_2$ and $5s15d\ ^3D_2$, respectively. The reason for the abrupt disappearance of the $6sns\ ^1S_0$ series after $n = 15$ is not yet understood. It would have been interesting had we observed some other $J = 0$ levels in this region of spectrum so that an MQDT type analysis could be done. Similarly, the interpretation of the multiplet around 23730 cm^{-1} is $5s17d\ ^1D_2$, and an overlapping contour of $4d6s\ ^3D_2$ and $5s17d\ ^3D_2$ lines, respectively. As a result of this interaction, the $5snd\ ^3D_2$ series at higher n-values gains oscillator strength at the expense of the $5snd\ ^1D_2$ series members. An identical intensity variation has been noted in the absorption spectrum of magnesium [25] mercury [26] and ytterbium [27] which is attributed to a transition from the LS to jj-coupling with the increase of the principal quantum number n.

The interpretation of the $5snd\ ^{1,3}D_2$ levels has always been based on the MQDT analysis of Esherick [7], who observed these series using the two-photon excitation scheme in conjunction with the thermionic diode detector. A five-channel MQDT analysis was employed to investigate the series interactions among the $J = 2$ channels and it was inferred that the lower members of the $5snd\ ^1D_2$ series are perturbed by the $5p^2\ ^1D_2$ level and the higher members are influenced by the doubly excited $4d6s$ levels leading to a strong singlet-triplet mixing. Subsequently, Dai [15] treated the singlet and the triplet series separately using a two-channel MQDT model for the singlet series and a three-channel model for the triplet series.

Due to the presence of interlopers of the singlet and triplet characters, the interactions of the $5snd\ ^1D_2$ and $5snd\ ^3D_2$ can be treated as two independent two-channel models. It is worth mentioning that the present situation is not comparable to that of the barium $6snd\ ^{3,1}D_2$ series where the interaction was due to the doubly excited $5d7d\ ^1D_2$ level and it was treated as a three-channel model [28]. Beigang and Schmidt [13] inferred that a two-channel QDT analysis is sufficient to analyze the perturbation in the $5snd\ ^3D_{1,3}$ series in strontium. In order to present a comprehensive and consistent picture, we have performed the MQDT analysis for all the four series separately, in the perturbed region from $n = 9$ to 30, and demonstrate that even for the $5snd\ ^{1,3}D_2$ series, a two-channel analysis is sufficient to recapitulate the series perturbations. As a result, the perturbing levels $4d6s\ ^1D_2$ and $^3D_{1,2,3}$ are found to be heavily mixed and spread over the entire Rydberg series, therefore, the exact term energies of the perturbing levels cannot be given. However, from the calculated admixture coefficients, it is possible to locate the interlopers for each series.

The studies of the perturbations of the $5snd\ ^1D_2$ and $5snd\ ^3D_{1,2,3}$ series with the $4d6s\ ^1D_2$ and $4d6s\ ^3D_{1,2,3}$ levels are based on the formulation of the multi-channel quantum defect theory by Cooke and Cromer [29]. Since the details of the MQDT have been already worked out, we will give here only the equations necessary for the analysis of the perturbations. For the two-channel problem the MQDT equation is written as

$$\begin{vmatrix} \tan\pi(\nu_1+\delta_1) & R_{12} \\ R_{12} & \tan\pi(\nu_2+\delta_2) \end{vmatrix} = 0\,. \qquad (1)$$

Here δ_1 and δ_2 are points of maximum contribution of dissociation channels 1 and 2 and ν_1 and ν_2 are the effective quantum numbers related to the term energy of each level according to the Rydberg relation

$$E_n = I_i - \frac{Ry}{(n-\mu_\ell)} = I_i - \frac{Ry}{\nu_i^2}, \quad i = 1 \text{ and } 2\,. \qquad (2)$$

Here E_n is the term energy, Ry is the mass corrected Rydberg constant for strontium 109736.6 cm^{-1}, μ_ℓ is the quantum defect and I_i are the ionization limits. In order to extract the MQDT parameters, we identify the first channel, for each Rydberg series separately, as $5snd\ ^1D_2$, $^3D_{1,2,3}$ attached to the first ionization limit at 45932.19 cm^{-1} and the second channel $4d6s\ ^1D_2$ and $^3D_{1,2,3}$ attached to the second ionization limit at 60628 cm^{-1} (average of the spin orbit split $^2D_{3/2}$ and $^2D_{5/2}$ levels of the ion). Since the series limits are well established, the fractional parts of the effective quantum numbers ν_1 (mod 1) with respect to the first ionization limit are plotted against the effective quantum number ν_2 with respect to the second ionization limit. The analytical relations to determine the allowed energy levels from equations (1) and (2) are

$$\nu_1 = \frac{1}{\pi}\tan^{-1}\left(\frac{R_{12}^2}{\tan\pi(\nu_2+\delta_2)}\right) - \delta_1 \qquad (3)$$

and

$$\nu_1 = \nu_2\left[1 - \nu_2^2\frac{(I_2 - I_1)}{Ry}\right]^{-1/2}. \qquad (4)$$

The term energies are found by solving these two equations simultaneously.

The curve that passes through the experimental points yields the MQDT parameters that are collected in Table 2 for all the four series. The quantum defect plots for these series are shown in Figure 5 for the singlet and triplet channels, respectively.

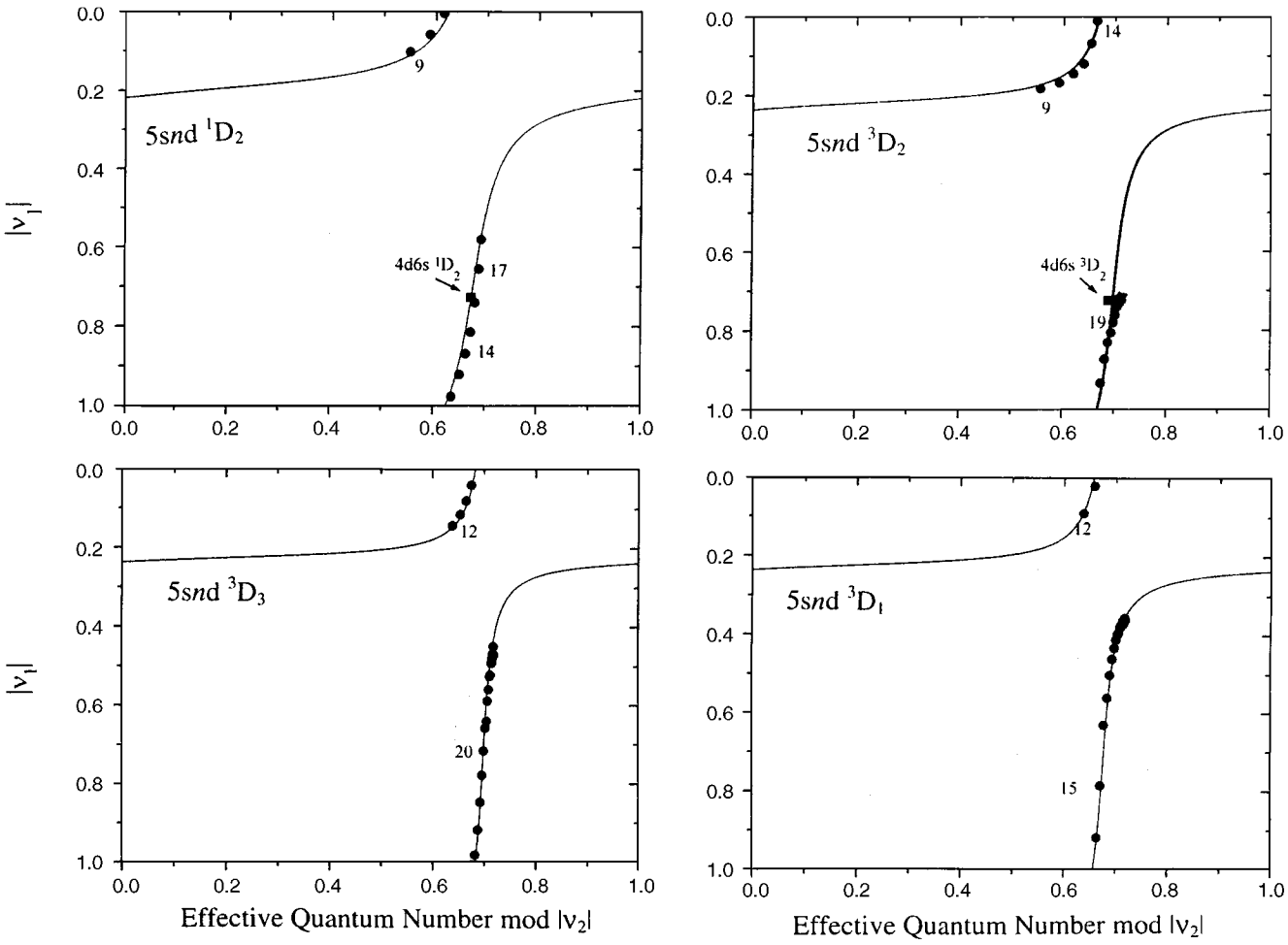

Fig. 5. Quantum defect plots for the $5snd\ ^1D_2$ and $5snd\ ^3D_{1,2,3}$ series of strontium. The data for the $5snd\ ^3D_{1,3}$ is taken from [9]. The $|\nu_1|$ is the effective quantum number with respect to the $5s\ ^2S_{1/2}$ first ionization threshold, while $|\nu_2|$ is the effective quantum number with respect to the $4d\ ^2D_{3/2,5/2}$ threshold. The regions of avoided crossings in all four plots reflect the nearly identical interchannel interactions.

Table 2. MQDT parameters for the $5snd\ ^1D_2$ and $^3D_{1,2,3}$ Rydberg series; $I_1 = 45932.19\ \mathrm{cm}^{-1}$, $I_2 = 60628.0\ \mathrm{cm}^{-1}$.

Rydberg Series	R_{12}	δ_1	δ_2
$5snd\ ^1D_2$	0.365	0.805	0.310
$5snd\ ^3D_3$	0.220	0.774	0.300
$5snd\ ^3D_2$	0.280	0.780	0.284
$5snd\ ^3D_1$	0.240	0.775	0.322

The admixture coefficients are given by the equations

$$|A_2|^2 = \frac{R_{12}^2(1+\tan^2\pi(\nu_2+\delta_2))}{R_{12}^4+\tan^2\pi(\nu_2+\delta_2)+R_{12}^2\{1+\tan^2\pi(\nu_2+\delta_2)\}}, \quad (5a)$$

$$|A_1|^2 = 1 - |A_2|^2 . \quad (5b)$$

The admixture coefficients of the $4d6s\ ^1D_2$, $^3D_{1,2,3}$ channels into the $5snd\ ^1D_2$, $^3D_{1,2,3}$ channels are shown in Figure 6. It is interesting to note that the mixing of the $4d6s$ $^1D_2$ and $^3D_{1,2,3}$ perturbing levels is not localized but they spread over the entire Rydberg series. That is why it had always been difficult to definitely assign a particular energy to the $^1D_2$ and $^3D_{1,2,3}$ levels belonging to the $4d6s$ configuration.

Ewart and Purdie [6] assigned the $4d6s\ ^3D_2$ at $45276.5\ \mathrm{cm}^{-1}$ and $4d6s\ ^1D_2$ at $45350.1\ \mathrm{cm}^{-1}$ that was energy degenerate with the $6s17\ ^1S_0$ level. Beigang *et al.* [30] considered it a localized perturbation and used $4d6s\ ^1D_2$ at $45056.1\ \mathrm{cm}^{-1}$ and $4d6s\ ^3D_2$ at $45367.4\ \mathrm{cm}^{-1}$ to analyze the perturbation in the $5snd\ ^1D_2$ series employing Languor's formula. As a result of this treatment some other levels were also assigned, particularly the $4d^2\ ^3P_2$ and the $5snd\ ^3D_2$ (n = 14-17) levels. Both these identified perturbers as $4d6s\ ^{1,3}D_2$ are either absent or too weak to be detected in the present experiment. Even if we take these levels as perturbers for the $5snd\ ^{1,3}D_2$ series they do not lie on the quantum defect plots, a basic criterium for the interchannel interactions.

The fact is that the $4d6s$ configuration based $^1D_2$, $^3D_{1,2,3}$ levels are heavily mixed with the $5snd\ ^1D_2$, $^3D_{1,2,3}$

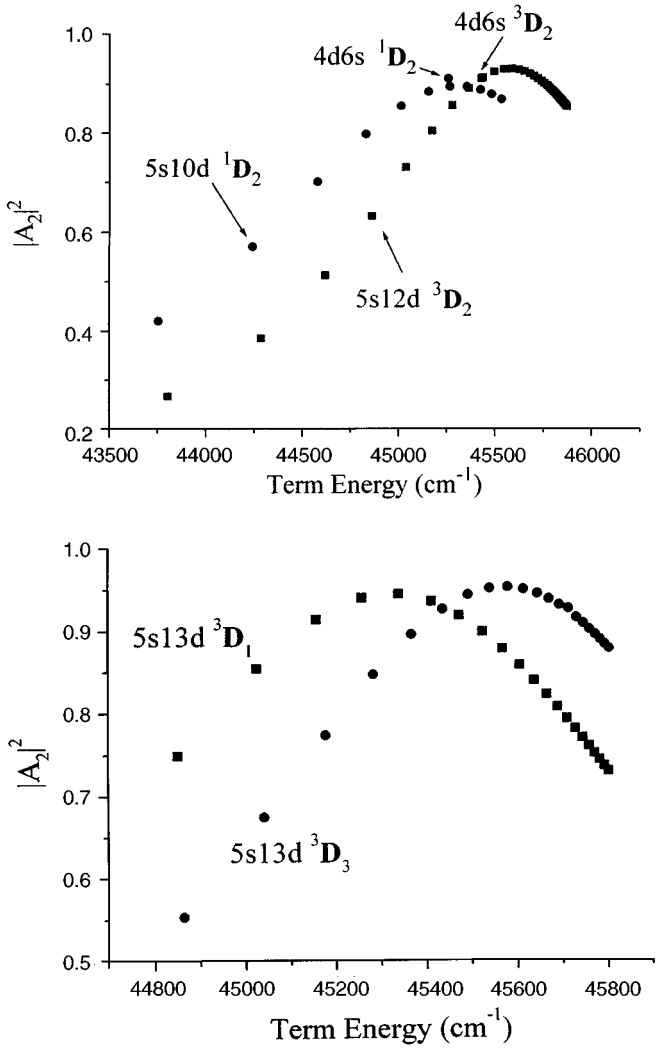

Fig. 6. Admixture coefficients $|A_2|^2$ of $4d6s\ ^{1,3}D_2$ channels in the $5snd\ ^{1,3}D_{1,2,3}$ series. The upper plot shows the admixture in the $5snd\ ^{1,3}D_2$ series and the lower plot shows the admixtures in the $5snd\ ^1D_2$ and $5snd\ ^3D_2$ channels. The extremely large mixing of the interlopers in the Rydberg series is the signature of the nonlocalized nature of the perturbations.

Rydberg series in strontium and lose their identity as individual levels. This fact is clearly reflected from the calculated admixture coefficients. In Table 3 (a,b,c,d) we present the term energies, admixture coefficients and effective quantum numbers for the $5snd\ ^1D_2$ and $5snd\ ^3D_{1,2,3}$ series, respectively. The mixing of the $4d6s\ ^1D_2$ level in the $5snd\ ^1D_2$ series is already 42% at $n = 9$, increases to 80% at $n = 12$, attains a maximum contribution of nearly 90% at $n = 16$ and then remains at a level of 88% at higher n-values. Therefore, if a definite assignment has to be provided for $4d6s\ ^1D_2$, the level at 45254.8 cm^{-1} is more probable which nearly contains 91% of its character. The situation is not very different for the interactions among the $5snd\ ^3D_2$ and $4d6s\ ^3D_2$ channels. The mixing of the $4d6s\ ^3D_2$ level starts from 27% at $n = 9$, approaches 89% at $n = 16$, maximum contribution of about

Table 3.a. Admixture coefficients $|A_i|^2$ for the $5snd\ ^1D_2$ and $4d6s\ ^1D_2$ channels. The level which can possibly be identified as $4d6s\ ^1D_2$ perturber is at 45254.8 cm^{-1} that contains the admixture of the channel 1 and 2, respectively, as 0.0881 and 0.9119. The other level observed in this energy region is $4d^2\ ^3P_2$ at 44729.6 cm^{-1} that was also reported in [7,30].

n	Term energy	$\|A_1\|^2$	$\|A_2\|^2$	ν_1
9	43756.0	0.5796	0.4204	7.101
10	44241.9	0.4297	0.5703	8.057
11	44578.6	0.2991	0.7009	9.004
12	44829.7	0.2018	0.7982	9.976
13	45011.8	0.1443	0.8557	10.920
14	45153.0	0.1150	0.8850	11.868
15	45263.6	0.1044	0.8956	12.813
16	45350.5	0.1048	0.8952	13.739
17	45421.0	0.1107	0.8893	14.654
18	45479.8	0.1196	0.8804	15.579

Table 3. b. Admixture coefficients $|A_i|^2$ for the $5snd\ ^3D_2$ and $4d6s\ ^3D_2$ channels. The level which can be identified as $4d6s\ ^3D_2$ perturber is at 45426.0 cm^{-1} that contains the admixture of the channels 1 and 2 as 0.0881 and 0.9119, respectively.

n	Term energy	$\|A_1\|^2$	$\|A_2\|^2$	ν_1
9	43804.7	0.7332	0.2668	7.182
10	44287.1	0.6154	0.3846	8.167
11	44619.8	0.4882	0.5118	9.144
12	44860.3	0.3680	0.6320	10.119
13	45036.7	0.2694	0.7306	11.067
14	45171.4	0.1947	0.8053	12.010
15	45276.5	0.1428	0.8572	12.933
16	45361.9	0.1079	0.8921	13.872
17	45433.0	0.0862	0.9138	14.829
18	45492.7	0.0742	0.9258	15.805
19	45542.2	0.0689	0.9311	16.779
20	45584.2	0.0680	0.9320	17.760
21	45619.7	0.0698	0.9302	18.739
22	45649.9	0.0733	0.9267	19.720
23	45676.6	0.0777	0.9223	20.730
24	45699.4	0.0825	0.9175	21.716
25	45719.4	0.0875	0.9125	22.722
26	45736.9	0.0924	0.9076	23.708
27	45752.2	0.0971	0.9029	24.705
28	45765.8	0.1016	0.8984	25.687
29	45778.1	0.1059	0.8941	26.685
30	45788.8	0.1099	0.8901	27.683

93% at $n = 21$ and then remains staggering at about 86% at higher n-values. In this case the level at 45426.0 cm^{-1} may be assigned as $4d6s\ ^3D_2$ and it lies on the quantum defect plot (see Fig. 5). A similar situation takes place for the $5snd\ ^3D_1$ and $5snd\ ^3D_3$ series. In the case of the $5snd\ ^3D_1$ series, a substantial mixing of about 75% of the $4d6s\ ^3D_1$ levels appears at $n = 12$ and it maximizes to 94% at $n = 16$ and then declines with still a large contribution of 73% at $n = 30$. Whereas, the $5snd\ ^3D_3$ series starts with a 55% mixing of the $4d6s\ ^3D_3$ level, maximum

Table 3.c. Admixture coefficients $|A_i|^2$ for the $5snd\ ^3D_1$ and $4d6s\ ^3D_1$ channels.

n	Term energy	$\|A_1\|^2$	$\|A_2\|^2$	ν_1
12	44854.02	0.2510	0.7490	10.089
13	45028.55	0.1454	0.8546	11.020
14	45159.6	0.0854	0.9146	11.918
15	45260.84	0.0594	0.9406	12.785
16	45324.36	0.0547	0.9453	13.628
17	45414.43	0.0635	0.9365	14.558
18	45475.35	0.0800	0.9200	15.499
19	45527.10	0.1001	0.8999	16.459
20	45570.97	0.1209	0.8791	17.430
21	45608.37	0.1410	0.8590	18.409
22	45640.43	0.1598	0.8402	19.394
23	45668.11	0.1769	0.8231	20.385
24	45692.08	0.1924	0.8076	21.378
25	45712.94	0.2062	0.7938	22.372
26	45731.28	0.2185	0.7815	23.371
27	45747.27	0.2295	0.7705	24.360
28	45761.60	0.2394	0.7606	25.363
29	45774.25	0.2482	0.7518	26.359
30	45785.48	0.2561	0.7439	27.349

Table 3.d. Admixture coefficients $|A_i|^2$ for the $5snd\ ^3D_3$ and $4d6s\ ^3D_3$ channels.

n	Term energy	$\|A_1\|^2$	$\|A_2\|^2$	ν_1
12	44865.22	0.4468	0.5532	10.141
13	45043.79	0.3259	0.6741	11.114
14	45180.44	0.2262	0.7738	12.082
15	45286.53	0.1528	0.8472	13.037
16	45370.76	0.1032	0.8968	13.981
17	45439.08	0.0725	0.9275	14.918
18	45495.02	0.0555	0.9445	15.844
19	45542.23	0.0477	0.9523	16.775
20	45582.38	0.0462	0.9538	17.712
21	45616.80	0.0488	0.9512	18.653
22	45647.54	0.0540	0.9460	19.635
23	45673.10	0.0604	0.9396	20.580
24	45695.94	0.0677	0.9323	21.552
25	45715.80	0.0752	0.9248	22.519
26	45733.69	0.0828	0.9172	23.512
27	45749.16	0.0900	0.9100	24.486
28	45763.12	0.0970	0.9030	25.477
29	45775.6	0.1036	0.8964	26.422
30	45786.61	0.1097	0.8903	27.455

mixing of 95% is around $n = 20$ and it remains reasonably high, 89%, at $n = 30$. From the purely maximum admixture coefficients, the term energies for the $4d6s\ ^1D_2$, $^3D_{1,2,3}$ levels may lie around 45280 cm^{-1}, 45340 cm^{-1}, 45590 cm^{-1}, and 45595 cm^{-1}, respectively. The observed levels at 45255 cm^{-1} and 45426 cm^{-1} are, therefore, tentatively assigned as $4d6s\ ^1D_2$ and $4d6s\ ^3D_2$, respectively.

Although our dye lasers were only 0.3 cm^{-1} broad, the observed widths of the lines are 1.5 to 3.0 cm^{-1}. We attribute this extra line width to the collisional broadening. We did not want to apply large fields to the plates to avoid any Stark effect. In order to achieve better signal-to-noise ratio, we had to raise the oven temperature, which produced high-density atomic beam. This way we achieved very good signal-to-noise ratio but at the expense of increased line widths.

In summary, by observing the molecular dissociative sequentially excited even parity $5snd\ ^{1,3}D\ J = 2$ Rydberg series from the $5s5p\ ^1P_1$ level in strontium, and presenting a consistent two-channel MQDT analysis for all four $5snd\ ^{1,3}D_{1,2,3}$ series we have shown that the perturbations between the $5snd\ ^{1,3}D_{1,2,3}$ channels and the $4d6s\ ^{1,3}D_{1,2,3}$ channels are not localized but these mutually perturbing channels are heavily mixed and lose their identity. Based on the calculated admixture coefficients, the $4d6s\ ^1D_2$ and $4d6s\ ^3D_2$ levels have been located at 45255 cm^{-1} and 45426 cm^{-1}, respectively. Term energies of a number of levels observed through direct two-photon excitation from the ground state and sequential excitation from the $5s5p\ ^1P_1$ resonance are presented. To our knowledge, these are the first measurements involving the molecular dissociation process in strontium.

It is a great pleasure to acknowledge fruitful discussions on the subject and the pleasant hospitality of Prof. Dr. Demtroeder at Kaiserslautern University, Germany. We thank the AvH (Germany), TWAS Trieste, Pakistan Science Foundation PSF(104) and the PAEC (Pakistan) for providing the financial support. M.Y. and R.A. are grateful to ICTP for providing scholarship under the ICAC scheme. M.A.B. is thankful to the Alexander von Humboldt Stiftung for financing the present visit to the Kaiserslautern University, Germany where the work was completed.

References

1. W.R.S. Garton, K. Codling, Proc. Phys. Soc. **86**, 1067 (1965).
2. M.A. Baig, J.P. Connerade, J. Phys. B: At. Mol. Opt. Phys. **17**, L271 (1984).
3. J.A. Armstrong, J.J. Wynne, P. Esherick, J. Opt. Soc. Am. A **69**, 211 (1979).
4. T.F. Gallagher, *Rydberg Atoms* (Cambridge University Press, 1994).
5. W. Demtroder, *Laser Spectroscopy* (Springer-Verlag, Berlin, 1998).
6. P. Ewart, A.F. Purdie, J. Phys. B: At. Mol. Opt. Phys. **9**, L437 (1976).
7. P. Esherick, Phys. Rev. A **15**, 1920 (1977).
8. J.J. Wynne, J.A. Armstrong, P. Esherick, Phys. Rev. Lett. **24**, 1520 (1977).
9. J.R. Rubbmark, S.A. Borgstrom, Phys. Scripta **18**, 196 (1978).
10. R. Beigang, K. Lucke, A. Schmidt, A. Timmermann, P.J. West, Phys. Scripta **26**, 183 (1982).
11. R. Beigang, E. Matthias, A. Timmermann, Phys. Rev. Lett. **47**, 326 (1981).
12. P. Grafstrom, Z.K. Jiang, G. Jonsson, C. Levinson, H. Lundberg, S. Svanberg, Phys. Rev. A. **27**, 947 (1983).
13. R. Beigang, A. Schmidt, Phys. Scripta **27**, 172 (1983).

14. C.J. Dai, J. Quantum Spectrosc. Radiat. Trans. **54**, 1019 (1995).
15. C.J. Dai, Phys. Rev. A **52**, 4416 (1996).
16. D. Hanna, P. Karkainen, R. Wyatt, Opt. Quantum Electron. **7**, 115 (1975).
17. U. Fano, Phys. Rev. **124**, 1866 (1961).
18. C.E. Moore *Atomic Energy Levels, NSRDS-NBS* (US Govt. Printing, 1971).
19. A.Boutassetta, A.R. Allouche, M. Aubert-Frecon, Phys. Rev. A **53**, 3845 (1996).
20. T.F. Gallagher, W.E. Cooke, Phys. Rev. Lett. **42**, 835 (1979).
21. D. Popescu, I. Popescu, J. Maurer, C.B. Collins, B.W. Johnson, Phys. Rev. A. **12**, 1425 (1975).
22. M. Akram, R. Ali, M.A. Baig, Opt. Commun. **136**, 390 (1997).
23. M. Akram, M.A. Baig, J. Phys. B: At. Mol. Opt. Phys. **29**, L381 (1996).
24. M.A. Baig, M. Akram, S.A. Bhatti, N. Ahmad, J. Phys. B: At. Mol. Opt. Phys. **27**, L351 (1994).
25. M.A. Baig, J.P. Connerade, Proc. Roy. Soc. A **369**, 353 (1978).
26. M.A. Baig, R. Ali, S.A. Bhatti, J. Opt. Soc. Am. **14**, 731 (1997).
27. B. Alexa, J. Hormes, M.A. Baig, Bonn University unpublished report, (1984).
28. A. Giusti-Suzor, U. Fano, J. Phys. B: At. Mol. Opt. Phys. **17**, 215 (1984).
29. W.C. Cooke, C.L. Cromer, Phys. Rev. A. **32**, 2725 (1985).
30. R. Beigang, K. Lucke, A. Timmermann, P.J. West, D. Frolich, Opt. Commun. **42**, 19 (1982).